# Ray Methods for Internal Waves in the Atmosphere and Ocean

Dave Broutman,[1] James W. Rottman,[2]
and Stephen D. Eckermann[3]

[1]Computational Physics, Inc., Springfield, Virginia 22151;
email: daveb@uap2.nrl.navy.mil
[2]Department of Mechanical and Aerospace Engineering, University of California,
San Diego, La Jolla, California 92093; email: jrottman@ucsd.edu
[3]E.O. Hulburt Center for Space Research, Naval Research Laboratory, Code 7646,
Washington, D.C. 20375; email: eckerman@uap2.nrl.navy.mil

**Key Words**   ray theory, caustics

■ **Abstract**   We review the use of ray models for internal waves, particularly formulations for calculating wave amplitudes along the ray. These are expressed in spatial, wave number, and phase-space coordinates. The choice of formulation affects not only the difficulty of the calculations for rays and caustics but also the degree to which the waves satisfy slowly varying assumptions. We describe several examples taken from atmospheric and oceanic applications that illustrate the variety of options for ray models.

## 1. INTRODUCTION

Ray models are the basis for much of our understanding of atmospheric and oceanic internal waves. They describe the wave field that emerges from various sources, the subsequent propagation through a nonuniform background, and the approach to dissipation. Ray models also represent some of the leading attempts to account for internal-wave spectra and internal-wave dissipation rates in parts of the atmosphere and ocean, and they have been used to parameterize internal-wave drag in atmospheric circulation models. Here we review and relate ray models of internal waves for these and other applications. We concentrate on the formulation rather than on their predictions, a subject included in other surveys (e.g., Fritts & Alexander 2003).

Ray models can be formulated in spatial coordinates, in wave-number coordinates, or in a mix of the two. The formulation in wave-number coordinates is equivalent to the ray description of the Fourier transform of the wave field. However formulated, the wave amplitudes are controlled by the same basic rules of ray convergence and divergence, but some formulations are more convenient than

| 1. REPORT DATE **2004** | 2. REPORT TYPE | | 3. DATES COVERED **00-00-2004 to 00-00-2004** |
|---|---|---|---|
| 4. TITLE AND SUBTITLE **Ray Methods for Internal Waves in the Atmosphere and Ocean** | | | 5a. CONTRACT NUMBER |
| | | | 5b. GRANT NUMBER |
| | | | 5c. PROGRAM ELEMENT NUMBER |
| 6. AUTHOR(S) | | | 5d. PROJECT NUMBER |
| | | | 5e. TASK NUMBER |
| | | | 5f. WORK UNIT NUMBER |
| 7. PERFORMING ORGANIZATION NAME(S) AND ADDRESS(ES) **Naval Research Laboratory,E.O. Hulburt Center for Space Research,Washington,DC,20375** | | | 8. PERFORMING ORGANIZATION REPORT NUMBER |
| 9. SPONSORING/MONITORING AGENCY NAME(S) AND ADDRESS(ES) | | | 10. SPONSOR/MONITOR'S ACRONYM(S) |
| | | | 11. SPONSOR/MONITOR'S REPORT NUMBER(S) |
| 12. DISTRIBUTION/AVAILABILITY STATEMENT **Approved for public release; distribution unlimited** | | | |
| 13. SUPPLEMENTARY NOTES | | | |
| 14. ABSTRACT **see report** | | | |
| 15. SUBJECT TERMS | | | |

| 16. SECURITY CLASSIFICATION OF: | | | 17. LIMITATION OF ABSTRACT **Same as Report (SAR)** | 18. NUMBER OF PAGES **24** | 19a. NAME OF RESPONSIBLE PERSON |
|---|---|---|---|---|---|
| a. REPORT **unclassified** | b. ABSTRACT **unclassified** | c. THIS PAGE **unclassified** | | | |

others. For example, for a height-dependent horizontally uniform background, the transformation from horizontal spatial coordinates to horizontal wave-number coordinates straightens the rays and eliminates the more complicated occurrences of the ray singularity known as a caustic, so the ray calculation and the correction of the caustic can be made with relative ease.

A caustic is a singularity particular to ray theory. It occurs where neighboring rays intersect each other, resulting in an extreme breakdown of ray theory's slowly varying approximation and a ray prediction of infinite wave amplitudes. The familiar case is the buoyancy-frequency turning point (Lighthill 1978, section 4.11), where neighboring rays intersect as they reverse their vertical direction of propagation. This case is for a particular model and for a particular formulation of the ray equations. Typically, the caustic locations are more widespread, and in some models they can occur almost anywhere along the ray.

The problem with caustics is that their correction in numerical ray tracing is generally nontrivial. Very few of the models that we review correct any caustics at all. For some applications, such as those concerned with the approach to a critical layer, caustics are of limited interest. The rays may pass through a caustic on the way to a critical layer, but assuming no dissipation takes place at the caustic, it is enough to know that the amount of wave action carried by the waves is conserved through the caustic, and that ray theory becomes valid again after the ray leaves the caustic. In applications where caustics occur at locations of interest, the choice of model formulation can ease or obviate the correction of caustics. Part of the aim of this paper is to review how this has been done.

We start in Section 2 with a description of the spatial and wave-number formulations of ray theory. Initially we assume a steady source of waves in a steady background, as do many ray models of internal waves, but the general time-dependent ray equations for wave-amplitude calculations are also of interest and are described later in the section.

In Section 3 we discuss caustics. The familiar caustic at a buoyancy-frequency turning point is one case that can be handled easily, by a matching method or by a uniform approximation, usually involving an Airy function. The details are given in many other references (e.g., Kravtsov & Orlov 1999, Lighthill 1978), so we concentrate on another interesting example of a caustic that is less familiar but important in certain models of internal waves generated by flow over topography or by an oscillating source. Miles (1969) and Lighthill (1978) suggested alternatives to the basic ray method that avoid the difficulties in these respective examples. Miles's alternative is related to Maslov's method, the subject of Section 4.

Maslov's method takes advantage of the fact that the occurrence of caustics is formulation dependent. A caustic cannot occur along the ray in its spatial formulation and in its wave-number formulation at the same time. The idea in Maslov's method is to calculate the ray solution in the formulation without the caustic, and then to map it to a solution in the other formulation by Fourier transform. In theory, this corrects all types of caustics, and in some cases Maslov's method is actually easy to implement. We give an example in Section 4.

In Section 5 we discuss a range of applications that indicates the variety of options used in ray models for internal waves. Sometimes the formulation is chosen for the variables of direct interest, but the choice is also influenced by computational limitations and concerns about caustics. We do not cover basic internal-wave theory, which can be found in texts such as Gossard & Hooke (1975), Lighthill (1978), Gill (1982), and Nappo (2002). For other reviews of internal waves, see Fritts & Alexander (2003), McIntyre (2001), Baines (1995), Wurtele et al. (1996), and Muller et al. (1986).

## 2. GENERAL THEORY

Lighthill (1978, section 4.6) discusses the ray tracing of internal waves through a horizontal, vertically varying wind $U(z)$, directed along the $x-$axis. A ray is defined as the position $\mathbf{x}(t) = (x(t), y(t), z(t))$ that moves through the medium at the local group velocity of the waves $\mathbf{c}_g = (c_{g1}, c_{g2}, c_{g3})$ measured by a stationary observer on the ground. Because $U$ depends only on $z$, the horizontal wave numbers $k$, $l$ remain constant following the ray, as does the frequency $\omega$ measured by the stationary ground observer. The vertical wave number $m$ varies along the ray, as does the intrinsic frequency $\hat{\omega} = \omega - kU$ measured by an observer moving with the local wind velocity. For a single wave train of fixed $k$, $l$, $\omega$ and height-dependent $m(z)$, the wave amplitudes are predicted from the constancy of the wave-action flux $c_{g3}E/\hat{\omega}$, where $E$ is the wave-energy density (see Equation 19). This simple case explains aspects of phenomena such as the Booker-Bretherton critical-layer interaction (Gossard & Hooke 1975). To review other ray models of internal waves, we need to consider the more general theory.

The dispersion relation is $\omega(\mathbf{x}, t) = \Omega(\mathbf{k}, \mathbf{x}, t)$, for time $t$, position $\mathbf{x} = (x, y, z)$, and wave-number vector $\mathbf{k} = (k, l, m)$. The wave frequency is $\omega = \hat{\omega} + \mathbf{k} \cdot \mathbf{U}$, for intrinsic frequency $\hat{\omega}$ and a background velocity $\mathbf{U}$, which can vary in space and time. It is convenient to follow Hayes's notation (1970) for specifying the independent variables. When $\mathbf{k}$ and $\mathbf{x}$ are both treated as independent variables, we use $\Omega$ and partial derivatives denoted by subscripts. When $\mathbf{k}$ and $\mathbf{x}$ are treated as functions of one another, we use $\omega$ and partial derivatives denoted by $\partial/\partial t$, $\nabla \equiv (\partial/\partial x, \partial/\partial y, \partial/\partial z)$, and $\nabla_{\mathbf{k}} \equiv (\partial/\partial k, \partial/\partial l, \partial/\partial m)$. Notation such as $\Omega_{\mathbf{kk}}$ refers to the tensor with components $\Omega_{kk}$, $\Omega_{kl}$, etc.

The ray equations are (Lighthill 1978, Hayes 1970)

$$d\mathbf{x}/dt = \Omega_{\mathbf{k}} \tag{1}$$

$$d\mathbf{k}/dt = -\Omega_{\mathbf{x}}, \tag{2}$$

where $d/dt = \partial/\partial t + \mathbf{c}_g \cdot \nabla$ and $\mathbf{c}_g = \Omega_{\mathbf{k}}$ is the group velocity vector. There is no need yet to specify the form for $\Omega$, though for now we assume that $\Omega$ is independent of time. We relax this assumption later.

The ray equations for wave-amplitude calculations can be formulated in spatial coordinates or in wave-number coordinates. We first describe how these formulations are related to the ray phase-space formulation, where the independent coordinates are both **x** and **k**.

In phase space, the initial conditions uniquely determine each ray path, so there are no ray intersections and hence no caustics. Furthermore, the density of wave action in phase space is constant along the ray (e.g., Hertzog et al. 2002). Although the absence of caustics and the constancy of the wave-action density along the ray are nice simplifications, we are not usually interested in the phase-space density of wave action itself but rather in the spatial density or wave-number density of wave action. To obtain these densities, project the ray solution from phase space to the spatial domain or to the wave-number domain. In the projected domains, two neighboring rays can project onto the same point, resulting in a caustic.

Figure 1 illustrates the case where the projected rays form a caustic in the spatial domain. It is also possible to have a caustic in the wave-number domain, but an
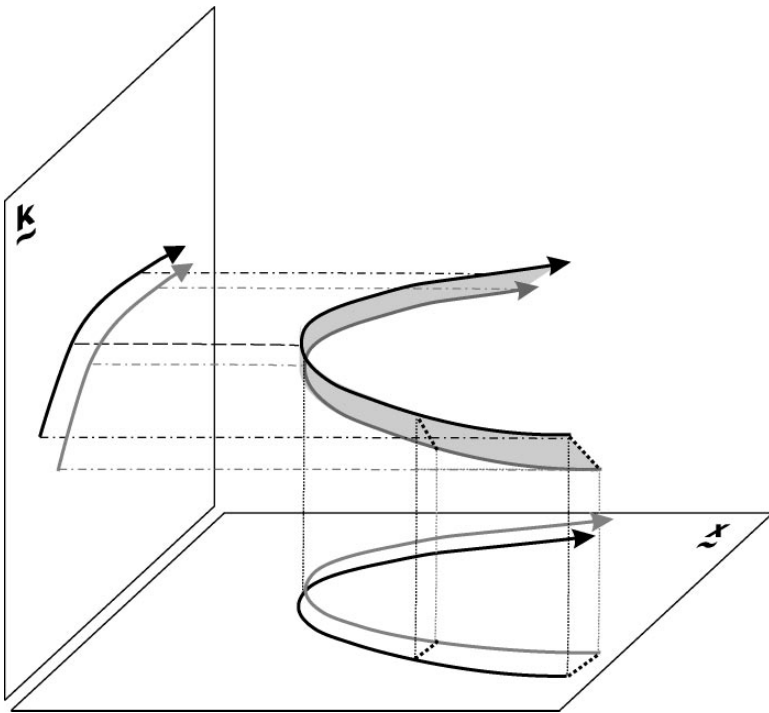


**Figure 1**   Rays in phase space are shown in this schematic diagram, along with their projections onto the spatial **x** domain and the wave-number **k** domain. Rays never intersect in phase space. Ray intersections, and hence caustics, occur only in the ray projections, in this case in the **x** domain.

important point is that a ray in phase space cannot simultaneously project onto a caustic in the wave-number domain and onto a caustic in the spatial domain. At a caustic in the spatial domain, neighboring rays have the same $\mathbf{x}$ but different $\mathbf{k}$. The situation is reversed at a caustic in the wave-number domain, where neighboring rays have the same $\mathbf{k}$ but different $\mathbf{x}$. If there were caustics in both domains simultaneously, the neighboring rays would have the same values of $\mathbf{x}$ and $\mathbf{k}$ and would not be distinct.

The ray solution for same quantity a($\mathbf{x}$t) in the spatial domain has the form

$$a(\mathbf{x}, t) = a_0(\mathbf{x})e^{i[\psi(\mathbf{x})-\omega t]}, \tag{3}$$

with $\mathbf{k}(\mathbf{x}) = \nabla\psi$. We assume for now a simple time dependence $e^{-i\omega t}$ with fixed frequency $\omega$. The corresponding ray solution in the wave-number domain is

$$b(\mathbf{k}, t) = b_0(\mathbf{k})e^{i[\phi(\mathbf{k})-\omega t]}, \tag{4}$$

with $\mathbf{x}(\mathbf{k}) = -\nabla_{\mathbf{k}}\phi$. The two phase functions $\phi$ and $\psi$ are related by the Legendre transformation (e.g., Brown 2000). Of more concern is the relation between the two amplitude functions $a_0$ and $b_0$, which is given by

$$a_0^2|\nabla_{\mathbf{k}}\mathbf{x}| = b_0^2. \tag{5}$$

The Jacobian $|\nabla_{\mathbf{k}}\mathbf{x}|$ is for the ray transformation $\mathbf{x}(\mathbf{k})$ that maps wave number to position.

At a caustic, the ray transformation $\mathbf{x}(\mathbf{k})$ is multivalued. In the case of Figure 1, two nonintersecting neighboring rays in the wave-number domain map onto the same spatial point $\mathbf{x}$ at the caustic, where the Jacobian vanishes:

$$|\nabla_{\mathbf{k}}\mathbf{x}| = 0. \tag{6}$$

Because $\mathbf{x} = -\nabla_{\mathbf{k}}\phi$ (see Equation 4), the Jacobian can also be expressed as $|\phi_{\mathbf{kk}}|$, a term that appears in the denominator of the amplitude of the stationary-phase solution (e.g., Shutts 1998, equation 65) and accounts for the breakdown of the stationary-phase method at a caustic. The stationary-phase condition is simply the ray transformation $\mathbf{x}(\mathbf{k})$.

In the following, we identify $a_0^2$ and $b_0^2$ with the wave-action densities in the spatial domain and in the wave-number domain, respectively. We continue to ignore time dependence (except in the wave phase). We invoke the idea of a narrow ray tube, which consists of a set of neighboring rays. The wave-action density within the ray tube is controlled by the convergence and divergence of neighboring rays that make up the ray tube (e.g., Lighthill 1978). Conservation of wave action implies that $\nabla \cdot (\mathbf{c}_g a_0^2) = 0$. Use of the Gauss divergence theorem then leads to the relation for the constancy of wave-action flux through the ray tube (e.g., Broad 1999).

$$a_0^2\, d\mathbf{x}/dt \cdot \hat{\mathbf{n}}\, dS = \text{constant}. \tag{7}$$

The constant here (and in the following three equations) is generally different for each ray tube. The group velocity is $\mathbf{c}_g = d\mathbf{x}/dt$, and $\hat{\mathbf{n}}\, dS$ is a directed area

element spanning the ray tube (e.g., Lighthill 1978, figure 89). An analogous solution exists for the wave-number domain:

$$b_0^2 d\mathbf{k}/dt \cdot \hat{\mathbf{n}} \, d\widetilde{S} = \text{constant},$$    (8)

where $\hat{\mathbf{n}} \, d\widetilde{S}$ is a directed area element spanning the ray tube in the wave-number domain. We return to Equation 8 in Section 5.3.

Two cases of Equation 7 are used commonly. In the first case, $\hat{\mathbf{n}}$ is parallel to $\mathbf{c}_g$, and $dS$ is the cross-sectional area of the ray tube. The left side of Equation 7 reduces to $a_0^2 |\mathbf{c}_g| dS$, as Lighthill (1978, p. 321) notes.

In the second case, $\hat{\mathbf{n}}$ is directed vertically, along the $z$ axis. Then $dS$ measures the area of a horizontal slice through the ray tube, and wave-action conservation becomes

$$a_0^2 c_{g3} J_1 = \text{constant}.$$    (9)

The Jacobian $J_1 = \partial(x, y)/\partial(x_0, y_0)$ is taken at fixed $z$ and is proportional to $dS$.

The vertical component of the group velocity is $c_{g3}$, and the coordinates $x_0$, $y_0$ refer to a reference position. [For a horizontally uniform background, it is sometimes convenient to use $k$, $l$ instead of $x_0$, $y_0$, as seen in Shutts (1998) and Broad (1999)].

If $J_1$ is constant, we are left with the constancy of $c_{g3} a_0^2$, the vertical flux of wave action. This has probably been the most widely used equation for wave-amplitude calculations in internal-wave models. The assumption (in addition to the neglect of time dependence) is that the horizontal divergence of the rays can be neglected.

So far, we have considered representations in spatial coordinates and in wave-number coordinates. It is sometimes convenient to mix the coordinates, e.g., to combine the vertical spatial coordinate $z$ with the horizontal wave-number coordinates $k$, $l$. All of the above relations generalize to this case in a natural way. For instance, the expression analogous to Equation 9 is

$$q_0{}^2 c_{g3} J_2 = \text{constant}.$$    (10)

Here the Jacobian $J_2 = \partial(k, l)/\partial(k_0, l_0)$ for reference values $k_0$, $l_0$; the wave-action density in $(k, l, z)$ is denoted by $q_0{}^2$. This form is especially useful for a horizontally uniform medium because the horizontal wave numbers are then constant along the ray, leaving $J_2 = 1$. In Section 4, we discuss the mapping of the ray solution associated with Equation 10 into a spatial solution by inverse Fourier transform.

Finally, we discuss ray formulations for the general case that includes full time dependence as well as full spatial dependence. The general expression for wave-action conservation, in the form of the ray equation, is

$$dA/dt = -A\nabla \cdot \mathbf{c}_g.$$    (11)

Here we use the notation $A$ (previously $a_0^2$ but now allowed to be time dependent) for the wave-action density in the spatial domain. Chain-rule differentiation of $\nabla \cdot \mathbf{c}_g$ leads to an expression involving the wave-number gradient tensor $\nabla \mathbf{k}$.

A separate ray equation for $\nabla\mathbf{k}$ can be derived (Hayes 1970), but elements of $\nabla\mathbf{k}$ diverge whenever the ray meets a caustic. So, near a caustic, Hayes (1970) suggests reformulating the ray equations in terms of $\nabla_{\mathbf{k}}\mathbf{x}$, the inverse of $\nabla\mathbf{k}$. This is in effect a mapping to the wave-number domain, which avoids the caustic in the spatial domain. Generally, there are also caustics in the wave-number domain, where $\nabla_{\mathbf{k}}\mathbf{x}$ diverges, so a ray-tracing scheme of this kind would need to alternate between formulations based on the two tensors $\nabla\mathbf{k}$ and $\nabla_{\mathbf{k}}\mathbf{x}$.

A single formulation is obtained from the parametric representation $\mathbf{x}(\mathbf{a}, t)$ and $\mathbf{k}(\mathbf{a}, t)$. Here $\mathbf{a}$, which has the same dimension as $\mathbf{x}$, is a label for each ray, for instance its initial position. The quantity of interest for the calculation of the spatial wave-action density $A$ is the Jacobian $J = |\nabla_{\mathbf{a}}\mathbf{x}|$, taken at fixed $t$, which measures the changing volume of an element of the ray tube advected along the ray at the local group velocity. At a caustic, $J$ vanishes so the ray integration can proceed through the caustic without dealing with singularity quantities such as $A$. The wave-action density is computed at positions before or after the caustic using the constancy of $AJ$ along the ray, though as Brown (2000) states, this does not alter the fact that the ray solution breaks down near the caustic. To obtain $J$, we need in the general case a ray equation for the nonsymmetric tensors $\nabla_{\mathbf{a}}\mathbf{x}$ and $\nabla_{\mathbf{a}}\mathbf{k}$ (Hayes 1970, White & Fornberg 1998):

$$d\nabla_{\mathbf{a}}\mathbf{x}/dt = \nabla_{\mathbf{a}}\mathbf{x} \cdot \Omega_{\mathbf{xk}} + \nabla_{\mathbf{a}}\mathbf{k} \cdot \Omega_{\mathbf{kk}} \tag{12}$$

$$d\nabla_{\mathbf{a}}\mathbf{k}/dt = -\nabla_{\mathbf{a}}\mathbf{x} \cdot \Omega_{\mathbf{xx}} - \nabla_{\mathbf{a}}\mathbf{k} \cdot \Omega_{\mathbf{kx}}. \tag{13}$$

These are derived from Equations 1 and 2 by applying the operator $\nabla_{\mathbf{a}}$. Note that $\nabla_{\mathbf{a}}$ and $d/dt$ commute, unlike $\nabla$ and $d/dt$. Similar equations have been used to assess the stability of trajectories in a Hamiltonian system (e.g., Gutzwiller 1990, p. 88). In some applications it is enough to know the total amount of wave action carried along with a group of waves. This amount is not dependent on the focusing of rays within the group and is constant following the group:

$$\int_{\mathcal{D}(t)} A(\mathbf{x}, t)\, d\mathbf{x} = \text{constant}. \tag{14}$$

The integral is taken over a volume $\mathcal{D}(t)$, whose boundaries move at the local group velocity. For an infinitesimally sized $\mathcal{D}(t)$, $A$ can be removed from the integral, and Equation 14 is equivalent to the constancy of $AJ$ along the ray. An analogous result holds for the wave-number domain:

$$\int_{\mathcal{K}(t)} B(\mathbf{k}, t)\, d\mathbf{k} = \text{constant}. \tag{15}$$

Here $B$ (previously $b_0^2$ but now allowed to be time dependent) is the wave-number density of wave action, and the integral is taken over a wave-number volume $\mathcal{K}(t)$ that moves with the rays in the wave-number domain. For a uniform medium, $\mathcal{K}$ has fixed size, independent of time, because $\mathbf{k}$ is constant along the ray. For more on volume integrals of this type, see Bühler et al. (1999).

In the rest of the paper we specialize to internal waves. We ignore non-Boussinesq effects, which are important in atmospheric applications but not for our discussion of ray formulations. We write the dispersion relation in the form

$$\omega = \hat{\omega} + \mathbf{k} \cdot \mathbf{U}, \tag{16}$$

where $\mathbf{U}(\mathbf{x}, t)$ is the background flow and $\hat{\omega}$ is the intrinsic frequency:

$$\hat{\omega} = \left(k_h^2 N^2 + m^2 f^2\right)^{1/2} / \left(k_h^2 + m^2\right)^{1/2} \tag{17}$$

The magnitude of the horizontal wave number is $k_h = (k^2 + l^2)^{1/2}$. The inertial (Coriolis) frequency is $f$ and the mean buoyancy frequency is $N$. In the hydrostatic limit without Coriolis effects, the dispersion relation reduces to

$$\hat{\omega} \approx \pm k_h N / m. \tag{18}$$

For internal waves the wave-energy density $E = A\hat{\omega}$ is related to the vertical displacement amplitude $\eta_0$ by

$$E = \frac{1}{2}\rho_0 \eta_0^2 \left(N^2 + f^2 m^2 / k_h^2\right), \tag{19}$$

where $\rho_0$ is the mean density.

## 3. CAUSTICS

The difference between ray theory and linear theory is that the former assumes slowly varying waves. The waves are not slowly varying in the vicinity of a caustic, defined as the line or surface containing points where neighboring rays intersect each other. The simplest caustic to analyze is flat, and correctable with an Airy function. The presence of caustic curvature complicates the numerical implementation of the caustic correction. Note that the Airy function solution for the curved caustic pictured in Lighthill (1978, figure 98) depends on the caustic curvature through the third derivative terms in Lighthill's equation 381. To determine the caustic curvature we need either to advect second derivatives of the wave number along the ray (in addition to the first derivatives in Equation 13, or to trace enough rays to map out the shape of the caustic. Neither appraoch is ideal for practical ray tracing. In addition, other types of caustics occur that are not treatable with an Airy function.

For example, consider the propagation of internal waves generated by flow over a mountain. Such mountain waves (reviewed by Wurtele et al. 1996 and Baines 1995) often grow to large amplitudes by the time they reach the stratosphere. Their dissipation is important for driving stratospheric winds, so the entire process of mountain-wave generation, propagation, and dissipation needs to be parameterized in circulation models that cannot adequately resolve the mountain waves. An early effort by Palmer et al. (1986) was based on a simple scheme designed by Lindzen
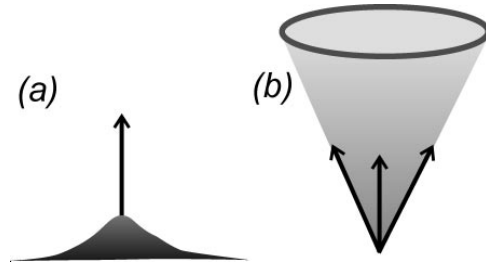
**Figure 2**    Two examples of an extreme breakdown of ray theory. The internal waves are generated by (*a*) flow over mountain and (*b*) a localized source of fixed frequency. All rays are confined to the vertical axis in (*a*) and to the surface of the cone in (*b*).

(1981). If we try to improve Lindzen's scheme using a standard ray method, the resulting ray prediction for the mountain-wave amplitudes is completely useless.

Lindzen treats the mountain waves as a single hydrostatic wave train that propagates directly upward above each mountain. The ray solution, on the other hand, includes rays for a spectrum of wave numbers, but in this case every ray follows the same path directly upward from the center of the mountain (Figure 2*a*). There is no horizontal propagation because the intrinsic horizontal group velocity of the mountain waves is directed upwind and is perfectly negated by the horizontal background wind. The ray prediction for the vertical displacement amplitude is infinite on the vertical axis, where there are infinitely many rays at each point, and zero at points off the vertical axis, where there are no rays.

A similar problem affects Lighthill's theory of waves emitted from a localized source (Lighthill 1978, section 4.9). The source has fixed frequency, and the background is stationary and uniform. Lighthill originally developed this theory for other types of waves. Its application to internal waves breaks down because all rays are constrained to the surface of a cone (Figure 2*b*). The ray prediction for the vertical displacement amplitude is infinite at points on the cone, where there are infinitely many rays at each point, and zero at points off the cone, where there are no rays. This cone is an example of a structurally unstable caustic, i.e., the caustic can be eliminated by a mere perturbation. For example, moving the source relative to the background, even at the slightest speed, spreads the rays off the cone and makes the ray prediction finite. This is exactly what Lighthill does in section 4.12 of his book. But a finite ray solution is still inaccurate if the rays do not separate sufficiently, and so the question arises: How fast do we have to move the source to get an accurate ray solution?

For the mountain-wave problem, the vertical line of rays above the mountain is also a structurally unstable caustic. Adding the slightest nonhydrostatic effects or Coriolis effects is enough to spread the rays downwind from the vertical axis and to give finite ray amplitudes. But again, unless these effects are significant, the ray solution in the important region directly over the mountain, at all heights, is

erroneously large because the rays are not well separated. Note that the only two-dimensional ray solution for mountain waves given in Baines (1995, p. 242) uses delta-function topography, which generates a strongly nonhydrostatic response. Similar problems occur in the three-dimensional case. Although some rays disperse downwind of the mountain in three dimensions, as part of a ship-wave pattern of lee waves, other rays remain strongly focused above the mountain. (See the singularity in the stationary-phase approximations of Smith 1980 and of Shutts 1998, and see figure 1*b* of Broutman et al. 2002).

The feature that distinguishes the Airy function caustic from the caustics mentioned above is the number of ray intersections. In the above cases, an infinite number of neighboring rays intersect at each point on the caustic. For the Airy function caustic, only two neighboring rays intersect at each point on the caustic. The Airy function caustic is structurally stable, a result predicted by catastrophe theory. For more on caustics as catastrophes, see Brown (2000), Kravtsov & Orlov (1999), and Nye (1999). [The amphidromic point in oceanographic tidal maps is another example of a structurally stable singularity of wave theory—see Nye's book (Nye 1999).] In the next section we describe a method that avoids the problem of these structurally unstable caustics without having to worry about the strength of the perturbation.

## 4. MASLOV'S METHOD

We note in the description of Figure 1 that one can avoid a caustic in the spatial domain by mapping the rays to the wave-number domain. The mapping separates the rays that intersect at a spatial caustic. Maslov's method uses the ray solution from one domain to correct the ray solution near caustics in the other domain. To review Maslov's method, we first consider the following three possibilities for transforming from the wave-number domain to the spatial domain:

| $\mathbf{k}$ − domain solution | | transform | | $\mathbf{x}$ − domain solution |
|---|---|---|---|---|
| *linear* | $\rightarrow$ | *IFT* | $\rightarrow$ | *linear* |
| *ray* | $\rightarrow$ | *ray* | $\rightarrow$ | *ray* |
| *ray* | $\rightarrow$ | *IFT* | $\rightarrow$ | *linear* (*approx.*) |

The first procedure is the usual Fourier-transform method, where IFT stands for the inverse Fourier transform. Because the ray solution is not used, there are no problems with caustics. But only a restrictive range of applications can be treated in this way due to the difficulty of finding the linear solution in the wave-number domain. The second procedure starts with the ray solution in the wave-number domain and maps it to the spatial domain using the ray mapping (or stationary-phase condition) $\mathbf{x}(\mathbf{k}, t)$. The ray mapping is multivalued at a caustic, where the ray

prediction gives infinite wave amplitudes. The third procedure is a combination of the first two. It starts with the ray solution in the wave-number domain and maps it to the spatial domain by IFT. For the moment, we assume that the ray solution in the wave-number domain is an accurate representation of the linear solution in the wave-number domain (which rules out caustics in the wave-number domain). The third procedure then gives an approximation to the linear spatial solution that is valid at all types of caustics in the spatial domain without further correction. The third procedure works at spatial caustics for the same reason that the first procedure works: the IFT superimposes all Fourier components to account automatically for diffraction as needed near any type of caustic. Away from the caustic there is the proper transition to the spatial ray solution, which appears automatically as the stationary-phase limit of the IFT.

Note that the IFT and the ray approximation do not commute. Taking the ray approximation after the IFT (a further step in the first procedure) yields the spatial ray solution that breaks down at the spatial caustics. Taking the ray approximation before the IFT (the third procedure) yields a solution that is valid at the spatial caustics, and elsewhere, again assuming that we start with an accurate ray approximation in the wave-number domain.

The third procedure is a simple example of Maslov's method. Consider the case of stationary mountain waves in a height-dependent background. It is convenient here to use the mixed formulation $k, l, z$, as in Equation 10. Maslov's solution for, say, the vertical displacement $\eta(\mathbf{x})$ is then

$$\eta(\mathbf{x}) = \iint \left[ \eta_0(k, l, z) e^{i \int_0^z m(k,l,z')dz'} \right] e^{ikx+ly} \, dk \, dl. \tag{20}$$

The term in square brackets is the ray solution in $k, l, z$ coordinates. Note that it has the ray-solution property that differentiation of the phase with respect to the independent variables $k, l, z$ gives the conjugate variables $-x, -y, m$. For differentiation with respect to $z$, this is obvious. For differentiation with respect to $k, l$, the result follows from $m_k = -dx/dz$, $m_l = -dy/dz$ (see Hayes 1970, equation 27a).

The amplitude $\eta_0$ in Equation 20 is determined from conservation of wave action in the form of Equation 10, and from the lower boundary condition at $z = 0$. For hydrostatic mountain waves, without the effects of Earth's rotation, Equation 20 becomes

$$\eta(\mathbf{x}) = \iint \left[ \hat{h}(k, l)[m(k, l, z)/m_0(k, l)]^{1/2} e^{i \int_0^z m(k,l,z')dz'} \right] e^{ikx+ly} \, dk \, dl. \tag{21}$$

Here $\hat{h}(k, l)$ is the Fourier transform of the mountain, and $m_0$ is the vertical wave number at the ground $z = 0$. For height-dependent $N(z)$, the integral in Equation 21 should be multiplied by $N(0)/N(z)$. Miles (1969, equation 4.13), Shutts (1998, equation 53), and Broutman et al. (2002, equation 27) derived solutions of this type. None of these studies accommodates trapped waves. Broutman et al. (2003) gives modifications for trapped waves and associated caustics.

Maslov's method also provides a solution for internal waves radiated from an oscillatory source, the problem described in the previous section. Lighthill (1978, section 4.10) treats this problem with a Fourier integral, but he reduces it to one dimension by applying the stationary-phase method in the other dimension (see equation 350 in Lighthill 1978). That makes Lighthill's solution a far-field approximation. Maslov's result is valid in the near field as well as in the far field. There is no distinction between the near field and the far field for the $k, l, z$ formulation because the rays are everywhere equally well separated by their values of $k, l$. Lighthill's solution is also restricted to a uniform background at rest with respect to the source, whereas Maslov's solution applies to a sufficiently smooth but otherwise arbitrary height-dependent background.

The difficult case for Maslov's method is when there are caustics in the wave-number domain as well as in the spatial domain. In some cases, it is straightforward to correct the caustics directly in the wave-number domain, before taking the IFT, as in Broutman et al. (2003). Alternatively, one can apply the IFT to ray solutions obtained in local regions of the wave-number domain where there are no caustics, as Maslov showed with an asymptotic theory. The result of the IFT then replaces the spatial ray solution, but only in regions surrounding the spatial caustics. In other regions, the spatial ray solution is retained. It is not clear how practical such a procedure would be for internal waves, though Brown (2000) applied it successfully to surface gravity waves. Ziolkowski & Deschamps (1984) and Thomson & Chapman (1985) discuss other applications of Maslov's method. Maslov's original work, from the 1960s, is summarized by Maslov & Fedoriuk (1981).

# 5. APPLICATIONS

We now discuss a selection of applications, and we continue to stress ray formulations rather than ray results. We base the discussion on wave action, although in some models the related quantity known as pseudomomentum is of more interest (e.g., Warner & McIntyre 1996). The wave-action density is denoted by $A$ for the spatial formulation, and by $B$ for the spectral or mixed spatial/spectral formulation.

## 5.1. Shear-Generated Internal Waves that Reach the Mesosphere

Shear instability on the upper edge of the jet stream leads to mixing patches whose collapse excites internal waves. Those internal waves that reach the mesosphere (at altitudes of 50–90 km) are potentially important for driving mesospheric winds, as discussed by Bühler et al. (1999) and Bühler & McIntyre. They used a Fourier integral representation for the waves in the near field surrounding the mixing patch, assuming a uniform background, and a ray representation for the waves in the far field. The ray representation accounts for wave propagation through height-dependent winds. The main concern is with the total amount of wave action that reaches the mesosphere.

Ray paths for this model are plotted in Figure 3 using the wind profile of Bühler & McIntyre (1999), as indicated in the figure. The only rays that can reach the mesosphere through this wind are those that leave the source with an intrinsic group velocity in the positive $x$ and positive $z$ directions. The usual notation for internal waves (e.g., Gill 1982) is such that these rays have $k > 0$ and $m < 0$. The other rays are absorbed by critical layers or reflected by turning points at altitudes below the mesosphere.

The total amount of wave action emitted by the mixing patch and associated with rays that have a chance of propagating into the mesosphere is (compare with equation 27 in Bühler et al. 1999)

$$P = \int_{k>0} \int_{-\infty}^{+\infty} \int_{m<0} B(\mathbf{k}) \, dk \, dl \, dm. \tag{22}$$

Here $B$ is the wave-action density in the wave-number domain. For a uniform background, $B$ is independent of time, so $B$ and $P$ can be calculated from the initial conditions, i.e., from the Fourier transform of the initial configuration of the mixing patch. We have been stressing the difference between the wave-number and spatial formulations of ray theory. The spatial distribution of wave action is highly time dependent. The spatial rays are given by $\mathbf{x} = \mathbf{c}_g t$, so the spatial wave-action density is initially concentrated at a single point at the center of the mixing patch, before dispersing rapidly in all directions. The spatial ray solution is not valid near the mixing patch because the rays are not separated sufficiently. But in wave-number space, the rays are separated by their $\mathbf{k}$ values. When Bühler et al. (1999) calculated the near-field solution in Fourier space, they calculated the equivalent of the ray solution in the wave-number domain.

The total wave-action $P$ emitted by the mixing patch would be the total wave action received by the mesosphere, except that some waves are reflected from turning points before reaching the mesosphere, and all of the waves experience viscous and radiative damping, which is important at these altitudes. These effects need to be taken into account, and this is where ray tracing is useful.

Suppose we divide the spectrum $k > 0$ and $m < 0$ into contiguous wave-number sections, labeled $\mathcal{K}_i$ for $i = 1,2,3....$ If the wave-number sections are small enough, $\mathbf{k}$ is approximately uniform within each wave-number section. We can then associate one ray and one value of the spectral wave-action density $B$ with each wave-number section.

The wave action integrated over each wave-number section $\mathcal{K}_i$ is constant, as expressed by Equation 15, apart from damping effects that can be modeled by

$$dP_i/dt = -P_i \cdot [\text{damping terms}]. \tag{23}$$

Here $P_i = \int_{\mathcal{K}_i(t)} B d\mathbf{k}$. If the damping terms are parameterized as a function of $\mathbf{k}$, the ray integration of Equation 23 is simple. The convergence of rays is not a concern, as it would be in the calculation of $B$ itself, and caustics are irrelevant. At a caustic $B$ diverges but the size of the corresponding volume element $\mathcal{K}_i$ vanishes.

The integral $P_i$ remains finite and gives the proper ray prediction for the amount of wave action transported through the caustic.

The rays are integrated from the mixing patch to the mesosphere, and the total amount of damping acting on each $P_i$ is calculated. The damping factor, i.e., the ratio of the final $P_i$ to the initial $P_i$, is then used to multiply $B$ in the corresponding wave-number element of a discretized Equation 22. In this way, the near-field integral Equation 22 is modified to give the far-field wave action received by the mesosphere.

The only difference between the above approach and that of Bühler & McIntyre (1999) is that the latter used the phase-space representation of wave action $\mathcal{N}(\mathbf{k}, \mathbf{x}, t)$ in place of our wave-number integral $P_i$. Both $\mathcal{N}$ and $P_i$ share the property that for nondissipative propagation they are constant along the ray, unaffected by the convergence of neighboring rays.

To assess the validity of the slowly varying approximation, Bühler & McIntyre (1999) monitored the quantity $m^{-2} dm/dz$, where $dm/dz = (dm/dt)/(dz/dt)$. This is the best that can be done for the variables integrated in the model. The quantity evidently approximates $m^{-2} \partial m/\partial z$, the fractional change in $m$ over a distance of $m^{-1}$ (Lighthill 1978, equation 139). The smallness of this fractional change is the appropriate condition for slow variation in certain one-dimensional models. In more than one dimension the validity conditions presumably involve derivatives of the other wave-number components, but the general form for the conditions is not clear. Various conditions that we have tested, though sometimes helpful, do not generally give a reliable indication of where ray theory breaks down.

## 5.2. Mountain Waves

The simplest model of mountain waves is hydrostatic and two dimensional, and it results in the worst possible breakdown of the slowly varying approximation (see Section 3). All ray paths coincide on the vertical axis directly over the mountain. An alternative is to attempt to represent the average conditions over the mountain with a single ray tube. In the simplest arrangement, the ray tube has constant width and is directed vertically, and the wave-action flux $c_{g3} A$ is constant along the ray tube, until dissipation. This idea has been used in schemes for the parameterization of mountain-wave drag (see the review by Kim et al. 2003) and for operational mountain-wave forecasting (Bacmeister et al. 1994).

An improvement to this appoach is to use several rays and allow them to propagate laterally away from the mountain. The position of each ray is determined by ray tracing, but the calculation is kept simple by preserving the vertical flux of wave action $c_{g3} A$ for each ray, in the absence of dissipation. Some nonhydrostatic and/or three-dimensional effects can be incorporated in this way. Schoeberl (1985) and Dunkerton (1981) give examples of this. Eckermann & Preusse (1999) also used this approach to improve the forecast model of Bacmeister et al. (1994) with the ray-tracing code of Eckermann & Marks (1997).

The above studies do not include the effects of the horizontal divergence of the rays on the wave amplitudes. For an infinitesimal ray tube, the horizontal divergence is determined by a Jacobian, as in Equation 9. Shutts (1998) and Broad (1999) made calculations using Equation 9 to examine the approach of hydrostatic mountain waves to critical layers in three dimensions. They did not evaluate the constant in Equation 9 but still predicted relative changes in $A$ along the ray.

An alternative is to formulate the ray solution in $k, l, z$ and use Maslov's method. Figure 4 shows an example of Maslov's spatial solution for mountain waves over Scandinavia. The calculation was made by the authors in a NASA measurement program during January 2003. Vertical profiles (assumed horizontally uniform) for the mean winds and the mean density were obtained from a weather forecast model. Broutman et al. (2002) gives more details on the calculation of Maslov's solution.

For the nonhydrostatic case, the presence of trapped mountain waves complicates the calculation of the ray solution in both $x, y, z$ and $k, l, z$ because there are turning points where $\hat{\omega} = N$ and where $c_{g3} = 0$. We are used to thinking of such turning points as caustics (e.g., Lighthill 1978, p. 396), but this is only true of the $k, l, z$ formulation. The turning point is not a caustic in the spatial formulation because there cannot be simultaneous caustics in two different projections of the phase-space rays (Section 2).

To illustrate this point, Figure 5 shows the spatial rays for the same problem presented in Figure 1 of Wurtele et al. (1996), which is also described in Wurtele et al. (1987) and in Broutman et al. (2003). The mountain is centered at the origin, and the wind flows from left to right, increasing linearly with height. The rays do not intersect at a turning point, and hence the turning point is not a caustic in the $x, y, z$ formulation. The rays encounter caustics, which appear as approximately straight lines that slope upwards from the origin. Note that each ray reflects from its turning point at a position that is slightly to the right of the nearest caustic. For more on the caustics in this particular problem, see Broutman et al. (2003).

## 5.3. Models of Internal-Wave Spectra

We now consider models that combine ray methods with a statistical representation of the wave field. We start with a case from the ocean: the refraction of short internal waves by a spectrum of longer internal waves. Using ray methods for this problem began in earnest with the preliminary study of Henyey & Pomphrey (1983), and continued with Flatté et al. (1985), Henyey et al. (1986), and Sun & Kunze (1999). (See also the review by Muller et al. 1986). These studies implement Monte Carlo ray tracings involving the Garrett-Munk model spectrum (Garrett & Munk 1979), which approximates measurements from the ocean and which is used in two ways: to set the amplitudes of the background long waves, and to set the initial conditions for the short waves. The idea is to duplicate the Garrett-Munk model in the initial conditions, for short waves of relatively large wavelengths, and then to see if

the ray tracing duplicates the Garrett-Munk model at smaller scales, down to dissipative wavelengths. Also of interest is the flux of wave action through the spectrum, which is used to predict ocean-mixing rates resulting from internal-wave dissipation.

The long-wave background is variable in all three spatial dimensions and in time. This is not a serious complication for calculating ray paths, but it is a serious complication for calculating the wave-number density or spatial density of wave action along the ray. The ray tracing would require the initialization and integration of the full set of ray equations in Equations 12 and 13, and would undoubtedly lead to frequent occurrences of caustics.

Flatté et al. (1985), Henyey et al. (1986), and Sun & Kunze (1999) simplified the wave-amplitude calculation and eliminated caustics by defining the ray tube statistically. They assumed that the statistics represented an internal-wave spectrum that was stationary and horizontally isotropic.

To see how this works, consider the form of wave-action conservation

$$B(k_h, m)\, dk_h/dt\, \Delta m = \text{constant}, \tag{24}$$

where $B$ is the spectral wave-action density. This is a special case of Equation 8 for the constancy of the wave-action flux $b_0^2 d\mathbf{k}/dt \cdot \hat{\mathbf{n}}\, d\widetilde{S}$ along a ray tube in the wave-number domain. To obtain Equation 24 from Equation 8, $\hat{\mathbf{n}}$ is the direction of the horizontal wave-number axis, and the width of the ray tube $d\widetilde{S}$ is the vertical wave-number variation $\Delta m$ across the ray tube. It is then assumed that each term in Equation 24 can be represented by its averaged value.

For example, Sun & Kunze (1999) used this approach to estimate the flux of wave energy to short dissipative scales. Initial conditions are specified at the relatively large scale for the short waves of 1-km horizontal wavelength: the Garrett-Munk spectrum sets the initial average for $B$, the discretization of the Garrett-Munk spectrum determines the initial $\Delta m$, and various estimates are used to set the initial average value for $dk_h/dt$ (see Sun & Kunze, p. 2912). This determines the constant on the right side of Equation 24, i.e., the wave-action flux for each ray tube. The wave-energy flux is then calculated at a small dissipative scale by multiplying the wave-action flux by the short-wave intrinsic frequency $\hat{\omega}$ at that small scale. Here $\hat{\omega}$ is obtained by tracing individual rays through realizations of the Garrett-Munk background. The small dissipative scale was chosen to be 5-m vertical wavelength.

Figure 6 illustrates another point about these ocean ray models. The ray paths shown in this figure follow short-wave propagation through a vertically localized packet of inertia waves centered in the middle of the plot. A numerical solution for the short waves is also shown. When this figure was first published in Broutman et al. (1997), the main interest was in the initial encounter of the short waves with the inertia-wave packet, at times just after one inertia period. The permanent upturn of the rays after one pass through the inertia-wave packet and the absense of critical layers for the short waves were noted as special features of refraction by time-dependent shear.
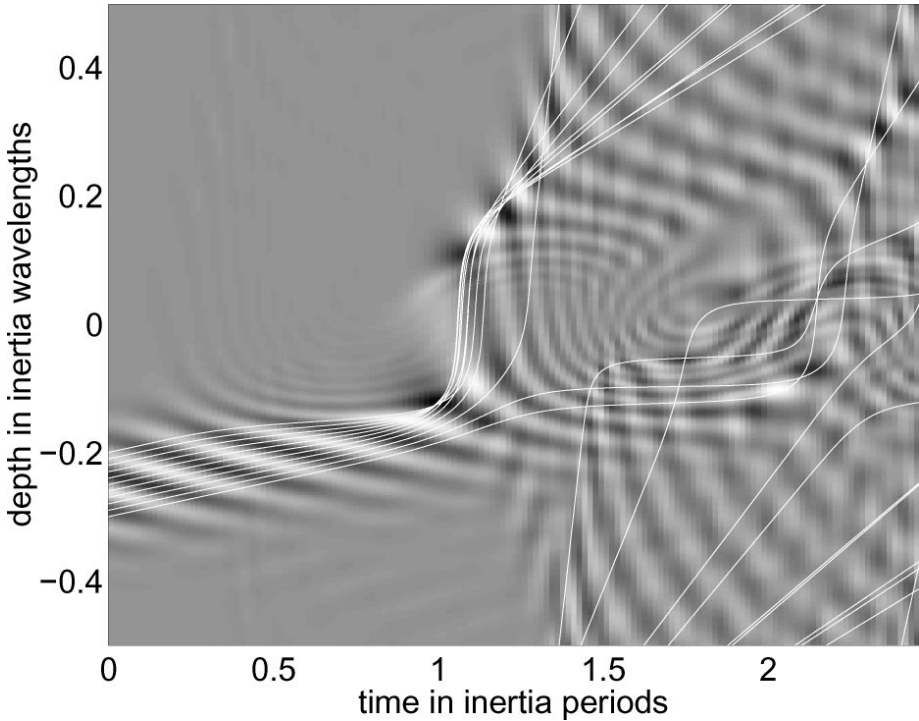
**Figure 6**   Ray paths and a numerical solution for short waves propagating through an inertia-wave packet. From Broutman et al. (1997).

Here we shift attention to earlier times. The short waves wrap around the periodic computational domain and repeatedly encounter the inertia-wave packet. The rays show signs of chaotic behavior, as they are likely to do in the models of Flatté et al. (1985), Henyey et al. (1986), and Sun & Kunze (1999). Henyey et al. (1986, section 2) noted that the individual rays in their calculations are very chaotic. However, the statistics that they derive from the individual rays appear to be very stable, and in good agreement with measurements. It may seem paradoxical that chaotic rays, with the sensitivities in tracing them, can yield stable and reliable results for the short-wave statistics, but this has been shown to occur in other studies of ray chaos, for example in acoustics and semiclassical physics (e.g., Brown et al. 2003).

Atmospheric refraction models have been developed with similar aims of predicting internal-wave spectra and dissipation rates. Warner & McIntyre's (1996, 1999, 2001) models are intended to be used for wave-drag parameterization in general circulation models and are thus constrained by computational costs to a much simpler design than the ocean models described above. For example, the refraction of short waves by long waves is ignored, and only the vertical variability

in the background winds is taken into account for the refraction. The rays are thus not chaotic, but the wave field is still represented statistically with a generalized wave packet, defined as a discrete element of the spectrum. Note also the use of wave-number (and frequency) coordinates in their ray formulation.

Hertzog et al. (2002) and Souprayen et al. (2001) give another statistical wave formulation. They use a phase-space representation to study the refraction of short internal waves by a spectrum of long internal waves in the atmosphere. They include the full space and time-dependence of the long waves in the ray tracing. The rays have numerous caustics when expressed in the spatial domain (appendix C of Hertzog et al. 2002), but as noted earlier the phase-space formulation is free of caustics and the phase-space density of wave-action $\mathcal{N}(\mathbf{k}, \mathbf{x}, t)$ is constant along the ray. Estimates of the energy spectrum in, say, $(m, z)$, are obtained by an integration of $\hat{\omega}N$ over $k, l, x, y$ (see equation 6 of Hertzog et al. 2002).

In models such as these, the rays wander quasi-randomly through large portions of the allowable phase space. The projection of the rays onto the spatial, wave-number, or mixed domains results in a dense concentration of caustics, and Maslov's method is not practical. The best hope of dealing with caustics in this situation is to smooth over them. The integration preformed by Hertzog et al. (2002) smoothes the caustics and seems to be similar in some respects to the treatment described in Berry (1983, section 3.4). Berry also gives a useful discussion of the representation of a wave field in phase space.

## 5.4. Other Applications

When the background is time varying, the ray-tube equations (Equations 7–10) are not applicable. Some models have been developed for a time-varying but spatially uniform background, e.g., Lott & Teitelbaum's (1993) mountain-wave study. They computed ray and caustic solutions from the stationary phase and Airy function limits of an integral representation. Ray-tracing models that describe time-dependent short-wave refraction by a single long-wave packet, or by a few long-wave packets, include Sonmor & Klaassen (2000), Eckermann (1997), Walterschied (2000), Zhong et al. (1996), Thorpe (1989), and Broutman & Young (1986). Sonmor & Klaassen (2000) gave a detailed analysis of short-wave caustics resulting from long-wave shear. Broutman & Young (1986) used a simple ray formulation involving the volume integral of wave action to identify a mechanism for the nondissipative damping of the long waves by the short waves. A more detailed calculation appeared in Broutman & Grimshaw (1988).

Horizontally varying backgrounds have been treated with ray methods for applications such as internal-wave propagation near fronts and vortices (e.g., Kunze 1985, Dunkerton 1984, Hertzog et al. 2001). Often, important insights are gained from an inspection of the ray paths without wave-amplitude calculations that would be complicated by caustics. Pringle & Brink (1999) provide a model with a tractable ray and Airy-function caustic calculation for internal waves over a sloping bottom in the presence of a horizontally sheared, depth-independent mean flow.

# 6. CONCLUSION

We discussed ray models for wave-amplitude calculations of internal waves, stressing ray formulations rather than ray results and practical implementations rather than formal theory. We gave examples that use spatial coordinates, wave-number coordinates, and phase-space coordinates, and that are expressed in terms of the local density or the volume integral of wave action. In most of these cases, the ray calculation is deterministic. In some cases, the wave amplitudes are initialized statistically and then followed along deterministic ray tubes (e.g., Warner & McIntyre 1996), and in other cases the wave amplitudes and the ray tubes are represented statistically (Henyey et al. 1986, Sun & Kunze 1999, Flatté et al. 1985).

The choice of ray formulation affects not only the difficulty of the ray calculation, but also the extent to which the waves satisfy slowly varying assumptions. For example, a spatial caustic can be mapped away by changing some or all of the spatial coordinates to wave-number coordinates. One formulation rarely suits the entire problem: the initialization, the ray tracing, the correction of caustics, the application of dissipative schemes, and the prediction of variables of interest. An aim of this paper has been to discuss how a combination of formulations and assumptions has contributed to the development of practical ray-tracing schemes.

**The *Annual Review of Fluid Mechanics* is online at http://fluid.annualreviews.org**

## LITERATURE CITED

Bacmeister JT, Newman PA, Gary BL, Chan RK. 1994. An algorithm for forecasting mountain wave–related turbulence in the stratosphere. *Weather Forecast.* 9:241–53

Baines PG. 1995. *Topographic Effects in Stratified Flows.* Cambridge, UK: Cambridge Univ. Press

Berry MV. 1983. Semiclassical mechanics of regular and irregular motion. In *Chaotic Behaviour of Deterministic Systems*, (Les Houches, Session 36), eds. G Iooss, RHG Hellerman, R Stora. Amsterdam: North Holland, pp. 171–271

Broad A. 1999. Do orographic gravity waves break in flows with uniform wind direction turning with height? *Q. J. R. Meteorol. Soc.* 125:1695–714

Broutman D, Grimshaw R. 1988. The energetics of the interaction between short small-amplitude internal waves and inertial waves. *J. Fluid Mech.* 196:93–106

Broutman D, Macaskill C, McIntyre ME, Rottman J. 1997. On Doppler-spreading models of internal waves. *Geophys. Res. Lett.* 24:2813–16

Broutman D, Rottman J, Eckermann SD. 2002. Maslov's method for stationary hydrostatic mountain waves. *Q. J. R. Meteor. Soc. B.* 128: 1159–72

Broutman D, Rottman J, Eckermann SD. 2003.

A simplified Fourier method for non-hydrostatic mountain waves. *J. Atmos. Sci.* In press

Broutman D, Young WR. 1986. On the interaction of small-scale oceanic internal waves with near-inertial waves. *J. Fluid Mech.* 166: 341–58

Brown MG. 2000. The Maslov integral representation of slowly varying dispersive wave-trains in inhomogeneous moving media. *Wave Motion* 32:247–66

Brown MG, Colosi JA, Tomsovic S, Virovlyansky AL, Wolfson MA, Zaslavsky GM. 2003. Ray dynamics in long-range deep ocean sound propagation. *J. Acoust. Soc. Am.* 113: 2533–47

Bühler O, McIntyre ME. 1999. On shear-generated gravity waves that reach the mesosphere. Part II: Wave propagation. *J. Atmos. Sci.* 56:3764–73

Bühler O, McIntyre ME, Scinocca JF. 1999. On shear-generated gravity waves that reach the mesosphere. Part I: Wave generation. *J. Atmos. Sci.* 56:3749–63

Dunkerton TJ. 1981. Wave transience in a compressible atmosphere. 1. Transient internal wave—mean flow interaction. *J. Atmos. Sci.* 38:281–97

Dunkerton TJ. 1984. Inertia gravity waves in the stratosphere. *J. Atmos. Sci.* 41:3396–404

Eckermann SD. 1997. Influence of wave propagation on the Doppler spreading of atmospheric gravity waves. *J. Atmos. Sci.* 54:2554–73

Eckermann SD, Marks C. 1997. GROGRAT: A new model of the global propagation and dissipation of atmospheric gravity waves. *Adv. Space Res.* 20:1253–56

Eckermann SD, Preusse P. 1999. Global measurements of stratospheric mountain waves from space. *Science* 286:1534–37

Flatté SM, Henyey FS, Wright JA. 1985. Eikonal calculations of short-wavelength internal-wave spectra. *J. Geophys. Res.* 90: 7625–72

Fritts D, Alexander MJ. 2003. Gravity wave dynamics and effects in the middle atmosphere. *Rev. Geophys.* 41 (doi:10.1029/2001RG000106)

Garrett CG, Munk WH. 1979. Internal waves in the ocean. *Annu. Rev. Fluid Mech.* 11:339–69

Gill AE. 1982. *Atmosphere-Ocean Dynamics.* New York: Academic

Gossard EE, Hooke WH. 1975. *Waves in the Atmosphere.* New York: Elsevier

Gutzwiller MC. 1990. *Chaos in Classical and Quantum Mechanics.* New York: Springer–Verlag

Hayes WD. 1970. Kinematic wave theory. *Proc. R. Soc. London Ser. A* 320:209–26

Henyey FS, Pomphrey N. 1983. Eikonal description of internal wave interactions: a non-diffusive picture of "induced diffusion." *Dyn. Atmos. Oceans* 7:189–219

Henyey FS, Wright J, Flatté SM. 1986. Energy and action flow through the internal wave field. *J. Geophys. Res.* 91:8487–95

Hertzog A, Souprayen C, Hauchercorne A. 2001. Observation and backward trajectory of an inertio-gravity wave in the lower stratosphere. *Ann. Geophys.* 19:1141–55

Hertzog A, Souprayen C, Hauchercorne A. 2002. Eikonal simulations for the formation and the maintenance of gravity wave spectra. *J. Geophys. Res.* 107:4145

Kim YJ, Eckermann SD, Chun HY. 2003. An overview of past, present, and future of gravity-wave drag parameterization for numerical climate and weather prediction models. *Atmos.-Ocean* 41:65–98

Kravtsov Y, Orlov Y. 1999. *Caustics, Catastophes, and Wave Fields.* New York: Springer-Verlag

Kunze E. 1985. Near-inertial wave propagation in geostrophic shear. *J. Phys. Oceanogr.* 15:544–65

Lighthill J. 1978. *Waves in Fluids.* Cambridge, UK: Cambridge Univ. Press

Lindzen RS. 1981. Turbulence and stress owing to gravity wave and tidal breakdown. *J. Geophys. Res.* 86:9707–14

Lott F, Teitelbaum H. 1993. Topographic waves generated by a transient wind. *J. Atmos. Sci.* 50:2607–24

Maslov VP, Fedoriuk ME. 1981. *Semi-classical*

*Approximation in Quantum Mechanics.* Holland: Reidel

McIntyre ME. 2001. Global effects of gravity waves in the middle atmosphere: a theoretical perspective. *Adv. Space Res.* 27:1723–36

Miles JW. 1969. Waves and wave drag in stratified flows. *Proc. 12th Int. Congr. Appl. Mech.*, ed. M Hetenyi, WG Vincenti, pp. 50–76. Berlin: Springer-Verlag

Muller P, Holloway GH, Henyey F, Pomphrey N. 1986. Nonlinear interactions among internal gravity waves. *Rev. Geophys.* 24:493–536

Nappo CJ. 2002. *An Introduction to Atmospheric Gravity Waves*. Academic Press. 276 pp.

Nye JF. 1999. *Natural Focusing and Fine Structure of Light.* Philadelphia: Inst. Phys.

Palmer TN, Shutts GJ, Swinbank R. 1986. Alleviation of a systematic westerly bias in circulation and numerical weather prediction models through an orographic gravity-wave drag parameterization. *Q. J. R. Meteor. Soc.* 112:1001–39

Pringle JM, Brink KH. 1999. High-frequency internal waves on a sloping shelf. *J. Geophys. Res.* 104:5283–99

Schoeberl MR. 1985. A ray tracing model of gravity wave propagation and breakdown in the middle atmosphere. *J. Geophys. Res.* 90:7999–8010

Shutts GJ. 1998. Stationary gravity-wave structure in flows with directional wind shear. *Q. J. R. Meteorol. Soc.* 124:1421–42

Smith RB. 1980. Linear theory of stratified hydrostatic flow past an isolated mountain. *Tellus* 32:348–64

Sonmor LJ, Klaassen GP. 2000. Mechanisms of gravity wave focusing in the middle atmosphere. *J. Atmos. Sci.* 57:493–510

Souprayen C, Vanneste J, Hertzog A, Hauchecorne A. 2001. Atmospheric gravity wave spectra: a stochastic approach. *J. Geophys. Res.* 106:24071–86

Sun H, Kunze E. 1999. Internal wave-wave interactions. Part II: Spectral energy transfer and turbulence production. *J. Phys. Oceanogr.* 29:2905–19

Thomson CJ, Chapman CH. 1985. An introduction to Maslov's asymptotic method. *Geophys. J. R. Astron. Soc.* 83:143–68

Thorpe SA. 1989. The distortion of short internal waves produced by a long wave, with applications to ocean boundary mixing. *J. Fluid Mech.* 208:395–415

Walterscheid RL. 2000. Propagation of small-scale gravity waves through large-scale internal-wave fields: Eikonal effects at low-frequency approximation critical levels. *J. Geophys. Res.* 105:18027–37

Warner CD, McIntyre ME. 1996. On the propagation and dissipation of gravity wave spectra through a realistic middle atmosphere. *J. Atmos. Sci.* 53:3213–35

Warner CD, McIntyre ME. 1999. Toward an ultra-simple spectral gravity wave parameterization for general circulation models. *Earth Planets Space* 52:475–84

Warner CD, McIntyre ME. 2001. An ultra-simple spectral parameterization for non-orographic gravity waves. *J. Atmos. Sci.* 58:1837–57

White BS, Fornberg B. 1998. On the chance of freak waves at sea. *J. Fluid. Mech.* 355:113–38

Wurtele MG, Sharman RD, Datta A. 1996. Atmospheric lee waves. *Annu. Rev. Fluid Mech.* 28:429–76

Wurtele MG, Sharman RD, Keller TL. 1987. Analysis and simulation of a troposphere–stratosphere gravity wave model. Part 1. *J. Atmos. Sci.* 44:3269–81

Zhong L, Manson AH, Sonmor LJ, Meek CE. 1996. Gravity wave exclusion circles in background flows modulated by the semidiurnal tide. *Ann. Geophys.* 14:557–65

Ziolkowski RW, Deschamps GA. 1984. Asymptotic evaluation of high-frequency fields near a caustic: An introduction to Maslov's method. *Radio Sci.* 19:1001–25
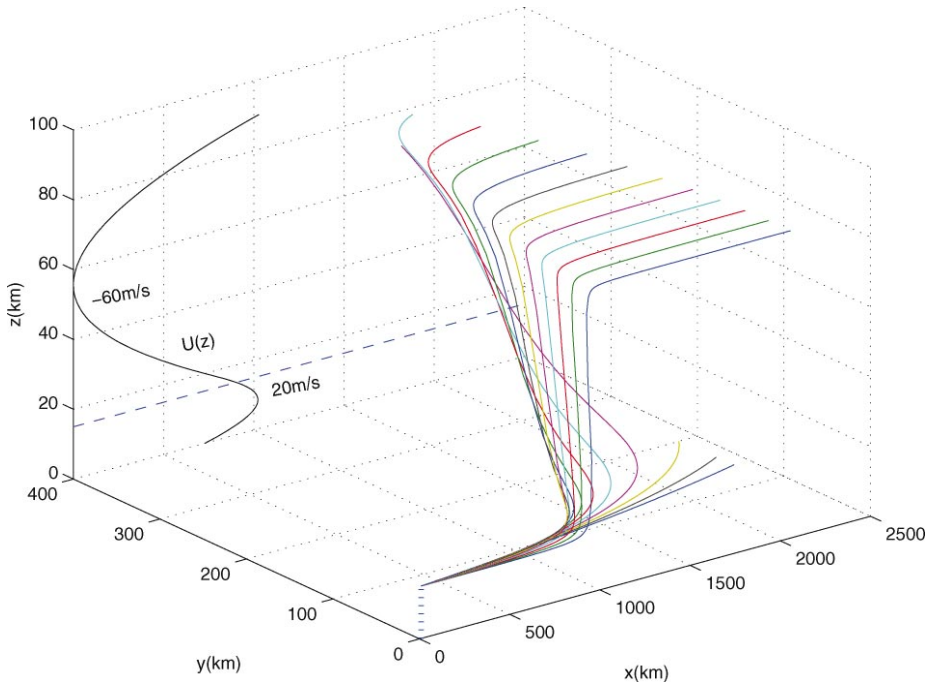
**Figure 3**  Ray paths for the Bühler-McIntyre model (Section 5.1) of internal-wave propagation from the upper edge of the jet stream through the stratosphere and into the mesosphere.
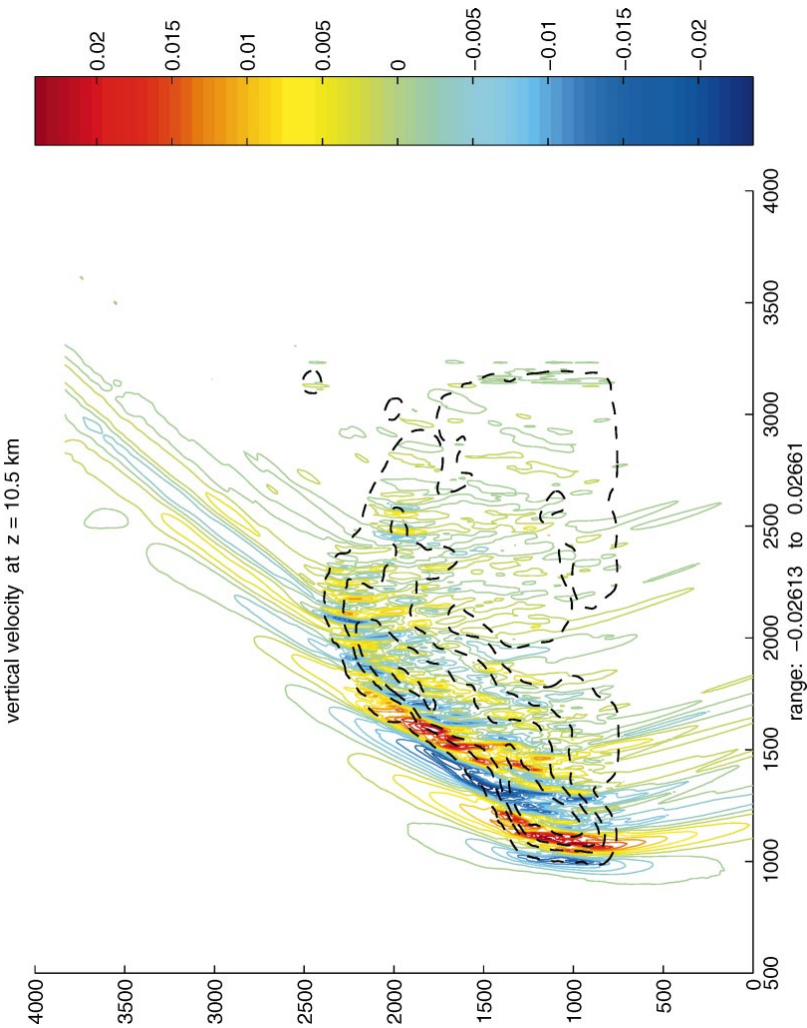
**Figure 4** The vertical velocity (in $ms^{-1}$) of mountain waves at a height of 10.5 km over Scandinavia. The result is calculated using Maslov's method, with Equation 20 approximated by a discrete Fourier transform on a 512 by 512 wave-number grid in $k$, $l$. The phase integral in Equation 20 is evaluated by a trapezoidal rule.
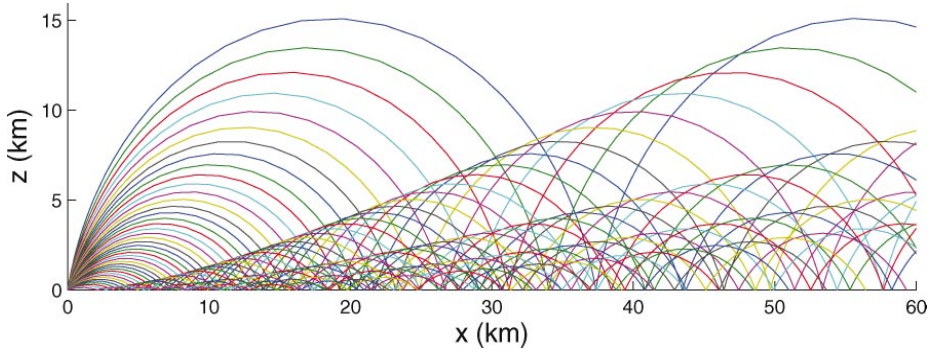
**Figure 5**   Ray paths for nonhydrostatic mountain waves.  The calculation corresponds to the model in figure 1 of Wurtele et al. (1996).  The mountain is centered at the origin, and the wind is in the positive $x$ direction and increases with height.